THIRTEENTH EUROPEAN ROTORCRAFT FORUM

78

Paper No. 92

CONSIDERATION OF TRENDS IN STABILITY AND CONTROL DERIVATIVES FROM HELICOPTER SYSTEM IDENTIFICATION.

C.G. BLACK
UNIVERSITY OF GLASGOW, U.K.

September 8-11, 1987
ARLES, FRANCE

ASSOCIATION AERONAUTIQUE ET ASTRONAUTIQUE DE FRANCE

ABSTRACT

This paper seeks to develop methods for the task of validating a complex non-linear model of helicopter dynamics against measured flight -data. The approach adopted here is to regard both the helicopter and the non-linear model as sources of data, and to measure the correspondence between them using a series of simplified descriptions, linearised for each flight condition. The aim is to achieve matching trends in parameter estimates for both these sources of data, as a justification for a validated model.

In order to obtain satisfactory parameter estimates for the matching of predicted and estimated trends, practical problems associated with the application of system-identification techniques to helicopters have to be overcome. These include difficulties caused by the ill-conditioning of the information matrix, which can result from correlations in the helicopter flight-data. In addition, for the use of a six-degrees-of-freedom model in the estimation, where the real system is of a higher order, there is a requirement to diminish or exclude the higher-order effects from the estimation. This may be achieved by the use of a restricted frequency range for the estimation, and by the incorporation of time delays into the model; both these are facilitated by the formulation of the estimation problem in the frequency domain.

Use is made of real flight-data obtained from flight trials with a Puma helicopter at RAE Bedford, for 60 and 100 knots nominal trim speeds. The simulated data are obtained from the HELISTAB model developed at RAE Bedford, and the estimation software was developed by the current author at Glasgow University.

NOMENCLATURE

A,B,H state matrix, control dispersion matrix, measurement transition matrix.
$A_{FF}, A_{FR}, \ldots B_F$ partition matrices of the 9DOF model relating fuselage and rotor effects.
a_{ij} elements of second order flapping equation.
a^*_{ij} elements of first order flapping equation.
$\underline{b}$ vector of constant biases im measurements.
c(t) general control.
$\underline{G}(\omega)$ correction term for transform of time derivative.
$\underline{g}$ gradient vector (output-error).
J cost function.
j complex number such that $j^2 = -1$
$\underline{k}$ vector of trim constants for measurements.
$L_v, L_r \ldots$ rolling moment derivatives.
M information matrix
$M_q, M_\omega \ldots$ pitching moment derivatives.
$N_v, N_r \ldots$ yawing moment derivatives.
p number of parameters estimated.
p(t),q(t),r(t) angular rates.
R theoretical ratio of parameter estimates.
S diagonal matrix of eigenvalues or singular values.
S error covariance matrix.
t time

$u(t), v(t), w(t)$ aircraft translational velocity components.
V_i eigenvectors.
V orthogonal matrix of eigenvectors.
$\underline{v}(t), \underline{V}(\omega)$ measurement noise - time domain and frequency domain.
X matrix of independent-variable values arranged in columns (equation-error method).
$\underline{x}(t), \underline{u}(t), \underline{u}^*(t,\tau), \underline{z}(t)$ state, control, extended control and measurement vectors (time domain).
$\underline{X}(\omega), \underline{U}(\omega), \underline{U}^*(\omega), \underline{Z}(\omega)$ state, control, extended control and measurement vectors (frequency domain).
X_R, X_F rotor state vector and fuselage state vector.
Y dependent variable (equation-error method).
$\alpha(t), \beta(t)$ incidence and flank angles.
$\beta_0, \beta_{1c}, \beta_{1s}$ coning, longitudinal and lateral cyclic flapping angles.
$\underline{\theta}, \Delta\underline{\theta}$ vector of unkown parameter estimates and increments.
$\underline{\phi}, \Delta\underline{\phi}$ linearly transformed vector of unknown parameter estimates and increments.
$\eta_0, \eta_{1s}, \eta_{1c}, \eta_T$ collective, longitudinal-cyclic, lateral-cylic and tail-rotor controls.
$\Delta\underline{\phi}(r)$ vector $\Delta\underline{\phi}$ with all but the first r elements set to zero.
$\underline{\varepsilon}(\omega)$ output-error vector.
τ time delay.
ω angular frequency.
ω_1, ω_2 angular frequency range used in estimation.
λ_i eigenvalues.
$[\ ]^T$ transpose.
$[\ ]^{-1}$ inverse.
$[\ ]^*$ transpose of complex conjugate.

(1) INTRODUCTION

Interest in the use of frequency-domain methods for aircraft parameter identification, in particular helicopter parameter identification, has increased during the last few years (e.g. refs. 6,12,17-19,21). Until recently, most published accounts were concerned with time-domain methods that used a reduced-order model representing six degrees-of-freedom rigid-body motion (refs. 4,13-16). A drawback with the time-domain approach is that the extension of the models used in the identification to include rotor degrees-of-freedom, results in a system of significantly higher order, and introduces severe difficulties in terms of the time-domain methods of identification.

In contrast, frequency-domain evaluation methods offer attractive possibilities in overcoming some of the problems associated with a direct use of the time domain in the estimation. The ability to define a frequency range over which the estimation is to be carried out is advantageous from the point of view of obtaining a reduced-order model valid over a certain frequency range, and in obtaining a reduction in the amount of data used in the estimation. In addition, the ability to estimate pure delays is facilitated by the formulation of the estimation problem in the frequency domain; the significance of this, and a demonstration of the improved model-fits and parameter estimates obtained as a result, will be shown in this paper.

The problems associated with helicopter parameter estimation are much greater than in the fixed-wing case. This is partly because of the increased complexity of the system (more degrees of freedom). Also the lengths of the records available for estimation are limited by the inherent instability of the helicopter, and the measurement signals may be heavily contaminated with noise because of the high-vibration environment. Difficulties are experienced in the application of parameter-estimation techniques when a high degree of correlation between the response variables exists; this is very much a problem with helicopter parameter estimation, and one which is addressed in this paper, through an investigation into the use of rank-deficient solutions for the output-error method.

The validation of theoretical helicopter flight-mechanics models is the primary motivation for the use of system identification techniques. The analyst is interested in both the estimated values themselves and the observed trends in the values for changes in the initial steady-state flight conditions about which the linear model is being considered. At the most basic level, the tendency of an important parameter to increase or decrease in value for changes in the nominal flight condition, is considered, and is compared with the direction of change (i.e. increase or decrease) predicted by the theoretical model. Next, the estimated values of the stability and control derivatives, for each of the flight conditions considered, can be compared directly with their theoretical counterparts; and when satisfactory agreement between theory and reality is obtained at this level, then some degree of validation of the theoretical model will have been obtained.

This paper seeks to build on the experience and confidence gained in the application of frequency-domain estimation techniques, and seeks to move towards the goal discussed in the previous paragraph. Use is made of real flight-data sets generated from lateral control inputs, and also of data generated from simulation models.

(2) THE ESTIMATION SCHEME

The estimation scheme used for the helicopter-system-identification work carried out at Glasgow University is shown in figure 1. There are three distinct steps in the estimation.

(1) A frequency-domain equation-error estimation, using singular-value decomposition, to obtain initial parameter estimates, and to determine insignificant parameters for exclusion from the estimation in the next stage. This step is implemented in a FORTRAN 77 program - SINGVAL, developed at Glasgow University.

(2) A frequency-domain output-error estimation implemented in a FORTRAN 77 program - OUTMOD, developed at Glasgow University; special features of this program include the ability to estimate delays in the controls and measurements, the ability to define relationships between different parts of the model structure during estimation, and the facility for rank-deficient solutions. The iterative optimization technique used is Gauss-Newton, with an additional scalar line-search improvement.

(3) A time-domain output-error estimation to obtain estimates of the zero offsets (including constant measurement biases), and initial

state conditions. The stability and control derivatives, and the estimated delays, are fixed during this estimation at the values estimated in stage 2. Time-domain verification of the model estimated in the frequency domain, is also provided at this stage, and is implemented in a FORTRAN 77 program - OFBIT, developed at Glasgow University.

Theoretical values are provided by the helicopter flight-mechanics simulation package HELISTAB (ref. 9), where the user specifies details of the required model, such as: flight condition, altitude conditions, degrees of freedom, etc.. In addition, the package can be used to generate simulated time responses on which an identification can be carried out; this is a useful feature for validating estimation techniques and software.

(3) APPLICATION TO FLIGHT DATA

(3.1) LATERAL STATE EQUATION USED IN ESTIMATION.

Consider the application of the estimation techniques to the estimation of lateral/directional parameters. The model used is as shown in 3.1, where the four lateral quantities: $v(t)$, $p(t)$, $\phi(t)$ and $r(t)$ constitute the state vector $\underline{x}(t)$. Longitudinal measurements: $\alpha(t)$ and $q(t)$, are incorporated together with the control input which is in use: $c(t)$, into an extended deterministic control vector: $\underline{u}^*(t,\tau) = (\alpha(t), q(t), c(t-\tau))^T$.

$$\dot{\underline{x}}(t) = A\,\underline{x}(t) + B\,\underline{u}^*(t,\tau) \qquad (3.1)$$

The control $c(t-\tau)$ represents either the lateral cyclic or pedal input, and a delay term τ has been included.

The measured variables are related to the state variables by the following linearised equation, where $\underline{K}$ and $\underline{b}$ represent zero offsets and constant biases respectively, and $\underline{v}(t)$ is the measurement noise.

$$\underline{z}(t) = H\,\underline{x}(t) + \underline{K} + \underline{b} + \underline{v}(t) \qquad (3.2)$$

Transforming into the frequency domain, and excluding $\omega=0$ from the range of frequencies used, results in the model.

$$j\omega\underline{X}(\omega) + \underline{G}(\omega) = A\,\underline{X}(\omega) + B\,\underline{U}^*(\omega) \qquad (3.3)$$

$$\underline{Z}(\omega) = H\,\underline{X}(\omega) + \underline{V}(\omega) \quad \omega\neq 0 \qquad (3.4)$$

$\underline{G}(\omega)$ in (3.3) is a correction term for the Fourier transform of a time-derived quantity which is not periodic within the data window considered. It arises from the approximation of the Fourier integral by the discrete Fourier transform (refs. 12,19,6).

Using the above model, estimates of the lateral stability and control derivatives, and the lateral-longitudinal cross-coupling derivatives, can be obtained by estimating elements of the A and B matrices. The maximum-likelihood cost function used for the estimation

has the form (ref. 21):

$$J = \sum_{\omega_1}^{\omega_2} (\underline{\varepsilon}(\omega)^* S^{-1} \underline{\varepsilon}(\omega) + \log_e |S|) \qquad (3.5)$$

Here $\underline{\varepsilon}(\omega)$ represents the difference between the observations and the model output in the frequency domain, S is the error covariance matrix, and ω_1-ω_2 is the range of frequencies used in the estimation. It is assumed that there is no process noise on the model.

(3.2) REVIEW OF EARLIER RESULTS AND PROBLEMS

Some previously published studies on helicopter parameter estimation have focused attention on some recurring themes in the results obtained. In reference 1, Padfield and DuVal, using the equation-error approach, present results, using flight data from a Puma helicopter with a nominal trim speed of 100 knots. These results illustrate a common failing in the use of six-degrees-of-freedom (6DOF) rigid-body models: that is the underestimation of primary rate damping derivatives such as pitch damping M_q and roll damping L_p. The authors of reference 1 point to similar results obtained by other researchers such as Molusis (refs. 2 & 3) and show that whilst some improvement is observed when the frequency content of the data is reduced, lessening the effects of the high-frequency rotor modes, the estimates are still unsatisfactory. These derivatives produce dominant effects about all axes, and should be predicted by relatively simple theory. A large underestimation of these important derivatives will consequently lead to a corruption of the estimates of other parameters in the model. It is therefore vital for the successful estimation of models from helicopter flight-data that large discrepancies between theory and predictions for these important parameters, be overcome.

It is thought that the main reason for the poor estimates of these parameters is connected with the quasi-static assumption about the behaviour of the main and tail rotors, inherent in a 6DOF rigid-body representation of the helicopter. It is assumed that the rotor can be tilted and instantaneously reaches a new trim position. In reality, however, there are some short term transient effects which manifest themselves in the rigid-body measurements through coupling, and this contamination results in a degradation of the estimates. The problem could conceivably be overcome by using longer data records in the estimation; however, practical difficulties associated with the stability of the helicopter prevent this.

One apparent solution to the problem would seem to be the inclusion of rotor states (e.g. for rotor flapping) in the model. This would require more measurements to be made, and more parameters to be identified, resulting in additional complexity in the estimation. An alternative route used by the current author, and one which particlarly lends itself to the frequency-domain output-error approach (ref. 5) is the use of delays in the controls to account for higher-order rotor effects in the estimation of 6DOF rigid-body models. In the application of this approach to the identification of longitudinal derivatives from flight-data, some success in obtaining improved model fits and parameter estimates, in particular for the pitching-moment damping M_q and control

sensitivity $M_{\eta_{1s}}$ have been obtained. The results are presented in reference 6.

Whilst the use of delays in some of the controls to account for higher-order effects with small time constants, leading to significantly improved model fits, was implemented on an empirical basis, it was subsequently found that Isermann (ref. 7) had suggested a similar simplification for reducing the number of parameters to be identified in single-input single-output transfer functions. This is consistent with the approach described before, since the modes associated primarily with main rotor/tail rotor states have time constants that are smaller in comparison to those of the rigid-body modes. The usefulness of delays in accounting for higher-order effects will be demonstrated later using simulated data generated from a 9DOF model that includes coning and flapping modes. Components of the identified delay could also result from a pure transport delay (ref. 19), and relative phase shifts present in the measurements.

In addition to the problem of the underestimation of the roll damping L_p, Padfield and DuVal's results obtained using the equation-error approach, show that the accompanying estimate of the derivative L_r was very high compared to theory. This anomaly has also been observed by the current author, for a range of flight conditions between 60 and 100 knots in level flight, using the equation-error approach.

If we consider the response (shown for the lateral variables as part of figures 7,8 and 9) to a pedal doublet input (shown in figure 2), for a Puma helicopter flying at a nominal trim level of 100 knots, in straight and level flight, altitude 6000 ft., it can be seen that there is a strong correlation between the roll and yaw rate responses. It can therefore be expected that difficulties in estimating some of the parameters associated with these variables will occur. The damped sinusoidal roll and yaw rate responses which are almost π radians out of phase with each other, and are associated with a 'Dutch-Roll' type mode.

The consequence of using non-orthogonal, indeed almost perfectly linearly dependent, responses in the estimation, can be understood when an attempt is made to formally invert the information matrix M, whether in the context of the equation-error approach:

$$\underline{\theta} = [X^TX]^{-1}X^T\underline{Y} = M^{-1}X^T\underline{Y} \qquad (3.6)$$

or in the context of the equation for update increments in the iterative output-error technique:

$$\Delta\underline{\theta} = M^{-1}\underline{g} \qquad (3.7)$$

It should be stressed that the above equations are not, of course, solved in practice by pre-multipication of the inverse. The inverse of the information matrix is a measure of the confidence in the estimates obtained, and because of the ill-conditioning of the matrix, numerical difficulties will be encountered in the practical implementation of any estimation algorithm. The information matrix will never be exactly singular, because round-off and other numerical errors prevent this from happening. Instead, all the eigenvalues of the information matrix will be non-zero, with the difference between the smallest and largest eigenvalues being many orders of magnitude.

(3.3) USE OF A RANK-DEFICIENT INFORMATION MATRIX IN THE OUTPUT-ERROR APPROACH

The use of singular-value decomposition in orthogonalising the independent-variable responses, for the equation-error approach, has been demonstrated and discussed by the current author using real flight-data in a previous paper (ref. 6). The use of a subset of the most significant orthogonalised independent variables, meant in effect that the most insignificant eigenvalues were removed from the information matrix, and this was shown to result in improved estimates in some cases.

The information matrix used in the iterative estimation technique, given by (3.7), can also be calculated with the most insignificant eigenvalues removed; this results in what is known as a rank-deficient solution (ref. 8).

In order to achieve rank-deficient solutions, consider a singular-value decomposition of the information matrix M, where for the special case of a pxp square symmetrical matrix (where p is the number of parameters requiring update increments), this corresponds to the eigenvalue-factorisation result often given in texts on linear algebra (e.g. ref. 20). This expression is given in (3.8); the diagonal matrix S (=Diag(λ_i)) will have the eigenvalues (i.e. the singular values) of M in descending order of magnitude down the leading diagonal, and the orthogonal matrix V will be composed of the eigenvectors V_i arranged in columns.

$$M = VSV^T \qquad (3.8)$$

Applying the above result to (3.7) we have:

$$VSV^T\Delta\underline{\theta} = -\underline{g} \qquad (3.9)$$

$$\rightarrow S\Delta\underline{\phi} = -V^T\underline{g} \qquad (3.10)$$

The diagonal nature of S allows (3.10) to be solved easily for the linearly-transformed set of parameter update increments.

$$\Delta\phi_i = (-V^T\underline{g})_i/\lambda_i \qquad (3.11)$$

By setting the most insignificant elements of the linearly-transformed update increment vector $\Delta\underline{\phi}$ (corresponding to small eigenvalues of M) to zero, and using the inverse of the linear transform to obtain the increments in terms of the original set of variables:

$$\Delta\underline{\theta} = V\Delta\underline{\phi}(r)$$

where $\Delta\underline{\phi}(r) = (\phi_1, \phi_2, \phi_3, \ldots \phi_r, 0, 0, 0)^T \qquad (3.12)$
we may obtain rank-deficient update increments.

For the symmetrical matrix M we can formally write the following expression for the inverse of a rank-deficient M:

$$M^{-1} = \sum_{i=1}^{p-r} \lambda_i^{-1}(V_iV_i^T) \qquad (3.13)$$

where r is the number of eigenvalues removed from the information matrix M. Whilst the above expression should not be used in calculating a rank -deficient M, it highlights the fact that the smallest eigenvalues are associated with directions in the parameter space that have the most uncertainty associated with them.

Before results obtained in applying this technique for the identification of lateral derivatives are presented, it is worth noting that in addition to the problems resulting from linear dependence, the information matrix will also be 'near singular' if one, or more, of the parameters to be estimated are weakly defined. In terms of the cost-function surface defined in the parameter space, this means that in the vicinity of the minimum, the surface is relatively flat in at least one direction; a relatively insignificant change in the cost-function value would occur for a relatively large change in the parameter value. For an iterative estimation scheme, using a rank-deficient information matrix, the final estimate of a weakly-defined parameter may depend very much on the initial guess. Consequently, weak or insignificant parameters should be excluded from the estimation at the outset; insight into the system, or significance measures (ref. 6) available at the equation-error stage can be used as a basis for judgement. In reference 11, the authors warn against the routine, or blind use of rank-deficiency in overcoming problems of uniqueness in the solution.

(3.4) APPLICATION TO REAL FLIGHT DATA - PUMA 100 KNOTS

Consider the pedal-doublet run described earler. The full-rank, and rank-deficient results, obtained using the frequency-domain output-error estimation technique described in references 5 and 6, are shown in Tables 1 a) & b). The results are also represented graphically for the important lateral derivatives, the delay, and the cost-function value in figure 3. Full-rank solutions with, and without, a delay in the control are also presented for comparison.

In total, 12 parameters were estimated for each of the rank-deficient solutions. The number of time-domain points input to the estimation program, and transformed into the frequency domain was 1700,sampled at 64 Hz., making a record of length 26.5625 seconds. The frequency range used in the estimation was 0.03765 - 0.4894 Hz., corresponding to 13 complex-valued frequency-domain points, and was chosen on the basis of magnitude plots of the Fourier transforms, obtained at the equation-error stage. Initial guesses for the parameters were also obtained at the equation-error stage, except for the delay which had an initial guess of zero.

The inclusion and estimation of a delay in the control, results in a substantially lower cost value at convergence. Figures 4 & 5 show the frequency-domain fits obtained for these two cases. The improvement obtained as a result of the delay is particularly visible for frequencies on either side of the peak at about 0.22 Hz. In general, the agreement between measured and predicted frequency-domain responses is very good, especially the rolling and yawing moment fits. The delay itself is estimated to be about 0.2 seconds, and has a relatively small error bound.

In the case of the rolling-moment parameters, the inclusion of a delay results in estimates that are in much better agreement with theory, than the case without the delay. As the rank of the solution is decreased to 9, there is a noticeable change in the estimates of L_v and L_r: L_v agrees very well with theory, whilst the L_r estimate is much closer to theory than the higher-rank cases. The roll damping L_p is lower than the theoretical prediction, but it is larger than corresponding estimates obtained from the equation-error approach (values of -0.9 and 0.86 for L_p and L_r respectively). The incorporation of a delay in the control has thus increased the estimate of L_p. The combination of the use of the output-error technique, the incorporation and estimation of a delay in the control, and the use of rank-deficiency in the information matrix - in particular for an information matrix of rank 9 - has led to rolling moment parameter estimates that are in generally good agreement with theory.

Consider now the yawing-moment derivatives: the rank-9 estimate of N_r is in excellent agreement with theory. N_p differs somewhat from theory, but is estimated with a relatively small error bound. N_v is estimated to be larger than the theoretical prediction, but is still of comparable magnitude. The pedal control sensitivity to yaw N_{ζ_p} is smaller than theory suggests; however, the estimate obtained from the rank-9 solution is the closest to theory. The frequency-domain fits obtained at convergence for the rank-9 solution are shown in figure 6. It can be seen that they are very similar to those for the full-rank case with delay presented in figure 5.

Following a frequency-domain estimation of the stability and control derivatives, the next stage in the identification scheme is to perform a time-domain output-error estimation to obtain estimates of the zero-offsets, constant biases in the measurements, and initial state conditions, with a view to obtaining a time-domain verification of the model identified in the frequency domain. This was done for the estimated model obtained in the following three cases: 1) full rank with no delay in the control 2) full rank with delay in the control and 3) rank-9 solution with delay in the control. The time-domain verification results following from the time-domain estimation are shown in figures 7 to 9. First comparing figures 7 and 8 for the full-rank solutions: it can be seen that for the roll rate channel in particular, the inclusion of the delay leads to a much tighter fit over the first few seconds of data, when the control input is applied; the rank-9 solution also shows this, and in comparison to the full rank case in figure 8, the time-domain fit is only slightly degraded towards the end of the time record.

The preference for the rank-9 solution was based on comparisons of the predicted theoretical values with corresponding estimates. It is accepted that all the parameter estimates obtained from flight data need not equal the theoretical values, since the purpose of system identification in the current context is both to confirm some aspects of the theoretical model, and to update others. However, as was mentioned earlier, important primary effects should be able to be predicted by relatively simple theory, and so the estimates of parameters strongly influencing these effects may be used as an indicator of how good the model is, alongwith the time-domain reconstructions and predictions of the model.

In going from rank 9 to rank 8 there is a substantial degradation in the estimates of most of the important parameters, such as: L_p, L_r and

N_r. Figure 10 shows for one iteration of the frequency-domain output-error method a typical reduction in cost-function value (normalised to the full-rank case) that would be obtained as the rank of the information matrix is increased from 1 up to the full-rank case. There is clearly a distinction between the rank-9, and rank-8 and lower-rank cost-reductions, whereas the rank-9 reduction is of comparable magnitude to the higher-rank cost-reductions. This observation seems to reflect the degradation observed in the parameter estimates for ranks lower than 9.

As described earlier, longitudinal measurements were included in an extended deterministic control vector for the four-state lateral model used in the estimation, with the significant cross coupling terms identified as elements of the control dispersion matrix B. Table 1 b) shows the values of the estimated lateral-longitudinal cross-coupling terms. In regard to the agreement with theory for these parameters, it can be seen that whilst there is not even any approximate matching, there is some evidence that rank-deficiency produces estimates which are at least of the correct order of magnitude. It can be appreciated that the degree of coupling-intensity between lateral and longitudinal states, in the 6DOF model, will determine the ease with which satisfactory estimates of these parameters can be obtained. As pointed out earlier, the use of rank-deficiency in situations where the information matrix is 'near singular' because of the presence of one or more weakly defined parameters, can result in situations where the estimates of the weak parameters are dependent on initial guesses. Indeed, for the current data set, there was found to be some evidence that for the cross-coupling terms, the rank-deficient solutions were dependent on the initial guesses, although estimates of the expected order of magnitude were still found. A contributory factor to the disagreement between estimates and theory for the cross-coupling terms could also be due to the fact that in directly incorporating longitudinal measurements into the extended control vector, the offsets relative to the centre of gravity of the corresponding measurement devices were not taken into consideration. In the case of the measurements that relate to the states in the linear model, offsets are accounted for through the measurement transition matrix H given in equations 3.2 and 3.4. For the extended control vector, this would require extra measurements to be included in the control vector, and extra parameters to be estimated in the B matrix.

It should also be noted that the use of noisy measurements - such as $\alpha(t)$ and $q(t)$ - as deterministic pseudo-controls is a possible source of error in the estimates, where in the estimation algorithm there is the inherent assumption that these are noise free. It is assumed that there is no process noise on the model. Larger models incorporating all longitudinal and lateral states would avoid the problem of noise on the controls, but would mean the estimation of a larger number of parameters, and would require the use data sets generated from control inputs that excite both the longitudinal and lateral modes: such data was not available for the current investigation.

(3.5) LATERAL CYCLIC INPUT - 60 KNOTS

Consider now the results obtained for a lateral-cyclic doublet input, for a Puma helicopter flying at a nominal trim level of 60 Knots,

in straight and level flight, altitude 1000 ft. .The input is shown in figure 11, and the lateral response variables are shown as part of figure 14. The length of record available for estimation is much shorter than in the previous case, with 800 points transformed into the frequency domain, sampled at 64 Hz., making a record of length 12.5 seconds. The frequency range used in the estimation was 0.08 to 0.56 Hz., corresponding to 7 complex-valued frequency-domain points.

The important lateral stability derivatives obtained from the frequency-domain output-error estimation are shown in figure 12 a), together with the estimates obtained from the previous 100-knots case, in order to clearly visualise any trends that may be apparent in the estimated values. Theoretical HELISTAB values are also shown for comparison. Error bounds are shown only for the rank-9 case in order to avoid the figure becoming too cluttered; the error bounds for the other cases are of a similar magnitude.

Concentrating first on the rolling-moment parameters, it can be observed that in the case of L_r the substantial improvement in the estimate that was obtained in the 100-knots case, as a result of using rank-deficiency, is not repeated for the 60-knots case; the lower-rank solutions are, however, smaller than the full-rank case. Once again, the estimate of L_v is improved by rank-deficiency, with the rank-10 and rank-9 estimates in excellent agreement with theory. The rank-10 and rank-9 estimates of L_p, whilst as with the 100-knots case are lower than theory, are consistent with the magnitude order predicted by theory.

For the yawing-moment derivatives, there is close agreement with theory for estimates of N_r, with the rank-10 and rank-9 solutions. A value higher than the theoretical prediction is obtained once again for N_p, though the value obtained for all the ranks is on the whole larger than the 100 knots-case, and this trend is predicted by theory. The Nv estimate is in excellent agreement with theory for the rank-10 case.

In figure 12 b) are shown estimates of the lateral-cyclic control sensitivity with respect to roll rate; the estimated delay in the control; and the final cost-function value at convergence. The rank-10 and rank-9 estimates of the control sensitivity are identical within the range of error. The estimated delay is not as large for the lateral-cyclic input as it was for the pedal input, and is not estimated with the same degree of confidence, although it is of a magnitude comparable to the time constant of the main-rotor longitudinal and lateral cyclic flapping modes.

It appears that for the lateral-cyclic case at 60 knots, the rank-10 solution gives the most satisfactory agreement with theory. The frequency-domain fits obtained at convergence for the rank-10 solution are shown in figure 13. In figure 14, the time-domain reconstruction is shown for the rank-10 estimates, following a time-domain output-error estimation of the zero offsets, and initial state conditions.

(3.6) TAIL-ROTOR - 60 KNOTS

Data obtained for a pedal-doublet input, for a Puma helicopter flying at a nominal trim level of 60 knots, in straight and level flight, altitude 1000 ft., was also analysed. The input is shown in figure 15. As with the 60-knots lateral-cyclic case, the length of record available for use was 12.5 seconds; this is considerably shorter

than the 26.5 seconds of data available for the 100-knots tail-rotor case. The magnitude of the doublet input, however, in this case is larger than the 100-knots case: the result being that the corresponding excursions from the nominal trim levels are large. This is not good for the estimation of a linearised model, and highlights an important point concerning control-input design: attention should be addressed not only to the shape or frequency content of any applied input signal, but also to its amplitude and the magnitudes of the excursions likely to be produced.

The frequency range used in the estimation was the same as the lateral-cyclic case - 0.08 to 0.56 Hz., corresponding to 7 complex-valued frequency-domain points. Estimates of the important lateral stability derivatives obtained from the frequency-domain output-error estimation are shown in figure 16. The full-rank case failed to converge, but by turning to rank-deficient solutions, convergence was obtained for the output-error method.

The results shown in figure 16 also include the estimates obtained for a full-rank solution when the L_r parameter is considered to be linearly related to L_p; the L_p parameter is estimated freely and the L_r estimate is constrained using the theoretical HELISTAB ratio of the two parameters:

$$L_r = R \, . \, L_p \qquad (3.14)$$

The result is that there are 11 free parameters to be estimated, and one additional related parameter which is updated at each iteration; the sensitivities are calculated within the output-error algorithm taking the defined relation into consideration. The ability to define relations between sets of parameters, is one of the features of the estimation program OUTMOD.

It can be seen that the cost-value obtained for the case with the relation between L_p and L_r is almost identical to the rank-11 cost-value obtained at convergence. In addition, the parameter estimates shown are identical, within the bounds of accuracy. For the rolling-moment parameters, there is good agreement with theory for L_v, L_p, and L_r, in both cases. In reality, the correlation is not usually between pairs of parameters, but may involve a large number of unknown parameters, and so the technique of fixing relationships between parameters is not a practical solution to the problem of correlations between parameters. The example shown, however, does perhaps reinforce earlier statements about likely problems in the estimation caused by strong correlations between the roll and yaw responses. The fact that for the results presented in the two previous cases, solutions of rank 9 and rank 10 respectively, gave the best estimates, where the full-rank case was of rank 12, does indicate that the existing correlations were indeed between more than simply L_p and L_r.

If we consider the yawing-moment parameters, it is seen that they are not estimated very well for the rank-11, and full-rank case with the defined relationship (i.e. rank 11), but require lower-rank solutions in order to approach the indicated theoretical values. On the whole, the estimated delay value is very similar to that obtained for the 100-knots tail-rotor case.

Comparing the cost-function values given in figures 16 and 12 b), it can be seen that for the 60-knots cases, they are, for all the rank-

deficient solutions presented, much greater for the pedal input than for the lateral-cyclic input. This is reflected in the better parameter estimates obtained in the latter case. It should be noted that the larger the cost value obtained at convergence, the poorer is the fit, and that comparisons of this type are valid here because the same number of frequency-domain points were used in the estimation process in both cases. It is felt that the large amplitude of the pedal input, and as a result, the less satisfactory adherence to the linear-model assumption of the responses are to blame for this.

(4) INVESTIGATION INTO THE USE OF TIME DELAYS USING 'HELISTAB'

HELISTAB (ref. 9) is a simulation flight-mechanics package developed at R.A.E Bedford, and which is currently installed at Glasgow University. It has options for a range of different rotor degrees-of-freedom, but the quasi-static rigid-body 6DOF model was used to supply the theoretical estimates presented in this paper for comparison with estimates from flight-data. The modifications required in the theoretical rigid-body 6DOF stability and control derivatives resulting from the neglect of the higher-order rotor dynamics (i.e. the quasi-static assumption) are discussed in reference 10.

The unforced tip-path plane motion of the rotor (without in-plane degrees of freedom) can be described by:

$$\dot{X}_R = A_{RR}\, X_R \qquad (4.1)$$

which in detail is:

$$\begin{vmatrix} \ddot{\beta}_0 \\ \ddot{\beta}_{1c} \\ \ddot{\beta}_{1s} \\ \dot{\beta}_0 \\ \dot{\beta}_{1c} \\ \dot{\beta}_{1s} \end{vmatrix} = \begin{vmatrix} a_{11}, a_{12}, a_{13}, a_{14}, a_{15}, a_{16} \\ a_{21}, a_{22}, a_{23}, a_{24}, a_{25}, a_{26} \\ a_{31}, a_{32}, a_{33}, a_{34}, a_{35}, a_{36} \\ a_{41}, a_{42}, a_{43}, a_{44}, a_{45}, a_{46} \\ a_{51}, a_{52}, a_{53}, a_{54}, a_{55}, a_{56} \\ a_{61}, a_{62}, a_{63}, a_{64}, a_{65}, a_{66} \end{vmatrix} \begin{vmatrix} \dot{\beta}_0 \\ \dot{\beta}_{1c} \\ \dot{\beta}_{1s} \\ \beta_0 \\ \beta_{1c} \\ \beta_{1s} \end{vmatrix} \qquad (4.2)$$

where β_0, β_{1c}, and β_{1s} are the coning, and longitudinal and lateral cyclic flapping angles.

The simplest approximation to the flapping motion is a 9 DOF model (6 rigid body + 3 flapping) obtained by setting the second-time derivatives of the left-hand side of (4.2) to zero; a procedure analagous to the setting of the rotor-state time derivatives to zero, to obtain expressions for the quasi-static rigid-body derivatives. The first-order approximation will finally have the form:

$$\begin{vmatrix} \dot{\beta}_0 \\ \dot{\beta}_{1c} \\ \dot{\beta}_{1s} \end{vmatrix} = \begin{vmatrix} a^*_{11}, a^*_{12}, a^*_{13} \\ a^*_{21}, a^*_{22}, a^*_{23} \\ a^*_{31}, a^*_{32}, a^*_{33} \end{vmatrix} \begin{vmatrix} \beta_0 \\ \beta_{1c} \\ \beta_{1s} \end{vmatrix} \qquad (4.3)$$

where the elements of the first-order flapping equation a^*_{ij} contain contributions from other elements in the matrix in (4.2), after a rearrangment of terms.

The full 9DOF model is described by:

$$\begin{vmatrix} \dot{X}_F \\ \dot{X}_R \end{vmatrix} = \begin{vmatrix} A_{FF} & A_{FR} \\ A_{RF} & A_{RR} \end{vmatrix} \begin{vmatrix} X_F \\ X_R \end{vmatrix} + \begin{vmatrix} B_F \\ B_R \end{vmatrix} U \qquad (4.4)$$

where $X_F = (u, w, q, \theta, v, p, \phi, r)^T$
$X_R = (\beta_0, \beta_{1c}, \beta_{1s})^T$
$U = (n_0, n_{1s}, n_{1c}, n_p)^T$

$A_{FF}, \ldots B_R$ are partitions of the stability and control matrices relating fuselage and rotor effects.

Consider a linear model of the form given in (4.4) with data generated using the program HELISTAB. The flight condition used was for level flight of 80 knots. The eigenvalues of the 11 x 11 system are given in Table 2.

The modes with small time constants (i.e. 1, 2&3, and 4) are associated mainly with the rotor-flapping states. Mode 1 is predominantly a coning mode, whilst modes 2&3 are associated with longitudinal and lateral cyclic flapping. Mode 4 has a relatively small eigenvalue in comparison to modes 1, 2&3.

Consider now the use of a reduced-order 6DOF model, having a time delay included in an active control, as an approximation to a 9DOF system. Stability and control derivatives were fixed at the quasi-static 6DOF values in a frequency-domain output-error estimation run, with the only free parameter in the estimation being the time delay. The simulated data used for the estimation run were generated from a 9 DOF system of the form given in (4.4).

The frequency range used in the estimation was 0 - 0.5 Hz., covering the range of the rigid-body modes. With this experiment, some indication of the requirement for a time delay in obtaining an improved model fit, for the reduced-order model can be established.

Consider first the application of longitudinal-cyclic doublets. The estimated delay as a function of sampling interval, is shown in figure 17 . For the one particular sampling interval of 0.015 seconds (approximately equal to the sampling interval of 0.015625 seconds for the flight-data), the estimated delay for each of the controls when a DFVLR '3211' input sequence is applied to that control alone, is shown.

As the results show, a positive time delay is strongly identified for the longitudinal-cyclic and lateral-cyclic inputs. For the longitudinal-cyclic doublet inputs, it is shown that as the sampling interval was increased, the estimated time delay decreased. This is because increasing the sampling interval effectively filters out the higher-order rotor effects. If the points in figure 17, representing the doublet inputs, are extrapolated to zero time delay, the corresponding sampling interval is very near to the time constant of 0.11 seconds for the longitudinal and lateral cyclic flapping modes - 2&3, given in Table 2.

The frequency-domain predictions, obtained from the rigid-body 6DOF model with time delay, for the data generated from the 9DOF model, for the same longitudinal-cyclic doublet input, are shown in figure 18. The corresponding comparisons of time-domain predictions for the 6DOF model, without and with the time delay, are shown in figures 19 a) and b). It

can be seen in this example, that a much closer match with the 9DOF data is obtained using the 6DOF model, when the time delay is included.

In the case of the collective input, the small value estimated for the delay, is probably connected with the coning mode (mode 1 in Table 2) which, in comparison to the longitudinal and lateral cyclic flapping modes, has a very small time constant. For the tail-rotor control there are no dynamics modelled in the HELISTAB program: the small delay estimated (less than the sampling interval) is the result of numerical noise. Results using real flight-data, some of which were discussed in detail earlier in this paper, have demonstrated the importance of having a delay associated with this control. For the longitudinal-cyclic '3211' input, the estimated delay is almost identical to that obtained for the doublet input.

These results have indicated that the inclusion of time delays, in some of the controls, is a very useful feature for the estimation of lower-order models, where the sampling interval is significantly less than the time constants of the important modes not included in the model; it is also much more satisfactory than increasing the sampling interval to a larger value.

(5) CONCLUSIONS

For the results presented in this paper, a number of observations can be made. Firstly, for the successful estimation of a rigid-body model, which excludes rotor degrees-of-freedom, the use of a frequency-domain output-error estimation technique has been shown to be a feasible and practical approach. Results for the estimation, from real flight-data, of lateral derivatives have been presented here; previous results for longitudinal derivatives were presented in reference 6. Secondly, some previously reported problems in the identification of lateral stability derivatives, associated with strong correlations between some of the response variables in the 'Dutch-roll' type mode, have been tackled using using rank-deficient versions of the information matrix. This has been shown to lead to marked improvements in the estimates of important lateral derivatives. The practical implementation of rank-deficiency, using a singular-value decomposition of the information matrix, in the output-error estimation method, has been discussed. The analogy which exists with the singular-value decomposition approach used in the equation-error method has been indicated. In addition, problems associated with the inclusion in the model for estimation of weakly defined parameters, when rank-deficient solutions are used, have been discussed.

Using both real flight-data, and simulated data generated from a 9DOF model, the improvement obtained in the model fits and parameter estimates by including a delay in the control to account for higher-order effects, where contamination of the data records used in the estimation of a reduced-order 6DOF model has a significantly degrading effect on the estimates, has been demonstrated.

Results were presented for 60 and 100 knots nominal flight conditions, and close agreement with theory was found for estimates of some of the important lateral parameters. Where the agreement with theory was not so close in the cases of N_p and L_p, the estimated error

bounds did, however, indicate a high degree of confidence in the estimated parameter values; also, in going from the 60 knots to 100 knots case, the predicted trend was for N_p to decrease, and L_p to increase, in magnitude, and this was found also in the estimation results for the selected rank-deficient solutions. The predicted and estimated trends in the case of L_v were in good agreement with theory, for the selected rank-deficient solutions; here the corresponding parameter values for the 60 and 100 knots cases matched well with theory. For a more thorough examination of predicted and estimated trends, it is felt that more high quality data would need to be available over a wider range of flight conditions; this is seen as an important future research task.

The results also brought out the importance of applying small-amplitude test input signals at the data collection stage in order to produce responses for which a linear model is a reasonable approximation, and which produce longer time records available for estimation; the most successful estimation was performed on the longest data record.

(6) ACKNOWLEDGEMENTS

The author should like to thank: Prof. David Murray-Smith of the Department of Electronics and Electrical Engineering, University of Glasgow; Mr. Roy Bradley of the Department of Aeronautics and Fluid Mechanics, University of Glasgow; and Dr. Gareth Padfield, Head of Helicopter Aeromechanics, Flight Research Division, RAE Bedford, for advice and help given in the preparation of this paper. The research on helicopter parameter identification carried out at the University of Glasgow is supported by the U.K. Ministry of Defence (Procurement Executive) through agreement No. 2048/028 XR/STR.

(7) REFERENCES

(1) G.D. Padfield, R.W. DuVal, Applications of system identification to the prediction of helicopter stability, control and handling characteristics. 'Helicopter Handling Qualities' NASA CP-2219, April 1982.

(2) J.A. Molusis, Rotorcraft derivative extraction from analytical models and flight test data. AGARD CP 172 'Methods for aircraft state and parameter identification', Nov. 1974.

(3) J.A. Molusis, Helicopter stability derivative extraction from flight data using the Bayesian approach to estimation. Journal of the AHS, July 1973.

(4) J.A. Molusis, Helicopter stability derivative extraction and data processing using Kalman filtering techniques. 28th AHS National Forum, Washington, 1972.

(5) C.G. Black, A frequency-domain output-error method of parameter estimation: development of method and computer implementation. University of Glasgow, GU Aero Report 8603, 1986.

(6) C.G. Black, D.J. Murray-Smith, G.D. Padfield, Experience with frequency-domain methods in helicopter system identification, 12th European Rotorcraft Forum, Garmisch, Federal Republic of Germany, 1986.

(7) R. Isermann, Identification of very noisy dynamic processes using models with few parameters, IFAC Identification and system parameter estimation, The Hague/Delft, 1973.

(8) D.E. Stepner, R.K. Mehra, Input design for identifying aircraft stability and control derivatives, NASA contractor report CR 220, March 1973.

(9) J. Smith, An analysis of helicopter flight mechanics: part 1 - users guide to the software package HELISTAB, RAE technical memorandum FS(B) 569, 1984.

(10) J. Kaletka, Rotorcraft identification experience, AGARD lecture series 104, parameter identification, 1979.

(11) R.E. Maine, K.W. Iliff, The theory and practice of estimating the accuracy of dynamic flight-determined coefficients: NASA reference publication 1077, 1981.

(12) K.H. Fu, M. Marchand, Helicopter system identification in the frequency domain, 9th European Rotorcraft Forum, Stresa, 1983.

(13) W.E. Hall Jr., N.K. Gupta, R.S. Hanson, Rotorcraft system identification techniques for handling qualities and stability and control evaluation, 34th AHS National Forum, Washington, May, 1978.

(14) R.W. DuVal, J.C. Wang, M.Y. Demiroz, A practical approach to rotorcraft system identification, 39th AHS National Forum, St. Louis, May, 1983.

(15) J. Kaletka, Practical aspects of helicopter parameter identification, AIAA Atmospheric Flight Mechanics Conference, Seattle, August, 1984.

(16) G.D. Padfield, R. Thorne, D.J. Murray-Smith, C.G. Black, A.E. Caldwell, UK researh into system identification for helicopter flight mechanics. 11th European Rotorcraft Forum, London, Sept., 1985.

(17) G.D. Padfield, Integrated system identification methodology for helicopter flight mechanics, 42nd AHS National Forum, Washington, June, 1986.

(18) M.B. Tischler, J.G.M Leung, D.C Dugan, Identification and verification of frequency domain models for XV-15 tilt-rotor aircraft dynamics. 10th European Rotorcraft Forum, The Hague, 1984.

(19) M. Marchand, K.H. Fu, Frequency domain parameter estimation of aeronautical systems without and with delay, IFAC Identification and System Parameter Estimation, York, UK, 1985.

(20) D.C. Murdoch, Linear Algebra, John Wiley and Sons, Inc., 1970.

(21) V. Klein, Maximum Likelihood Method for Estimating Airplane Stability and Control Parameters from Flight Data in Frequency Domain, NASA TR-1637, 1980.

Table 1a). Frequency-domain output-error estimates.
Pedal doublet input, Puma, 100 Kn, run R1201L.
Lateral derivatives (uncoupled).

Parameter	Full rank No delay	Full rank Delay	Rank 11	Rank 10	Rank 9	Rank 8	Theory
L_v	-0,0112	-0,0138	-0,0188	-0,0226	-0,0228	-0,0212	-0,022
	(0,0012)†	(0,0014)	(0,0016)	(0,0018)	(0,00076)	(0,00071)	
L_p	-1,317	-1,539	-1,408	-1,524	-1,491	-1,212	-2,05
	(0,14)	(0,14)	(0,17)	(0,19)	(0,042)	(0,041)	
L_r	1,237	1,097	0,748	0,563	0,444	0,965	0,294
	(0,13)	(0,13)	(0,16)	(0,099)	(0,044)	(0,039)	
$L_{\dot{v}}$	0,0455	0,0325	0,0229	0,0195	0,0174	0,0248	
	(0,0041)	(0,0044)	(0,0046)	(0,0052)	(0,0052)	(0,0050)	
N_v	0,00765	0,00865	0,00867	0,00822	0,00841	0,00728	0,00605
	(0,00056)	(0,00060)	(0,00063)	(0,00067)	(0,00061)	(0,00046)	
N_p	-0,353	-0,227	-0,254	-0,281	-0,283	-0,353	-0,0009
	(0,061)	(0,066)	(0,068)	(0,074)	(0,056)	(0,041)	
N_r	-0,494	-0,500	-0,518	-0,565	-0,525	-0,671	-0,528
	(0,062)	(0,062)	(0,067)	(0,057)	(0,058)	(0,017)	
$N_{\dot{v}}$	-0,0264	-0,0312	-0,0319	-0,0326	-0,0326	-0,0311	-0,043
	(0,0015)	(0,0014)	(0,0014)	(0,0016)	(0,0016)	(0,0014)	
$\tau(N_{\dot{v}})$	*	0,204	0,204	0,226	0,210	0,223	*
		(0,031)	(0,031)	(0,031)	(0,029)	(0,033)	
Cost value	-160,6	-178,9	-164,9	-153,7	-152,1	-148,4	*

Table 1b). Lateral/longitudinal cross-coupling derivatives.

L_α	-3,954	-3,700	-1,951	-0,839	-0,941	-0,200	≈-0,046
	(0,31)	(0,28)	(0,17)	(0,10)	(0,022)	(0,010)	
L_q	2,737	2,822	1,117	0,400	0,105	0,354	0,839
	(0,32)	(0,30)	(0,16)	(0,13)	(0,023)	(0,019)	
N_α	-0,0468	-0,304	-0,210	-0,308	-0,183	-0,400	-0,328
	(0,12)	(0,12)	(0,13)	(0,10)	(0,059)	(0,027)	

† estimated 1σ error bound.

Table 2. 9 DOF Eigenvalues.
HELISTAB Puma model, 80 Kn.

MODE	TIME CONSTANT (s)	REAL PART	IMAG. PART	MODULUS
1	0.033	-30.282	0.000	30.282
2	0.109	-9.190	5.224	10.571
3	0.109	-9.190	-5.224	10.571
4	0.478	-2.094	0.000	2.094
5		-0.961	0.724	1.203
6		-0.961	-0.724	1.203
7		-0.138	0.979	0.989
8		-0.138	-0.979	0.989
9		-0.00644	0.245	0.2454
10		-0.00644	-0.245	0.2454
11		-0.102	0.000	0.102

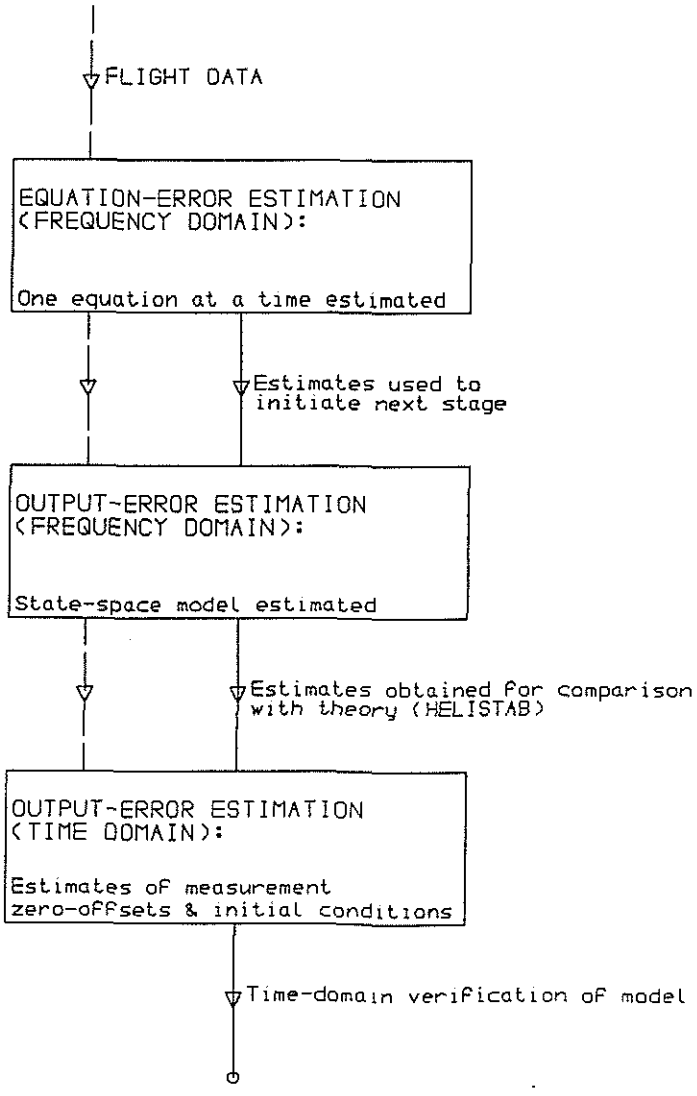

Figure 1. The Estimation sheme.

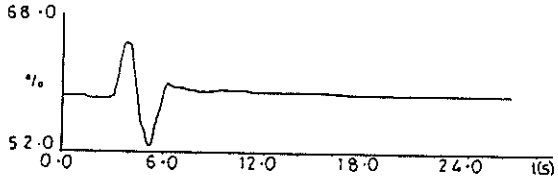

Figure 2. Pedal doublet input, Puma, 100 Kn, run R1201L.

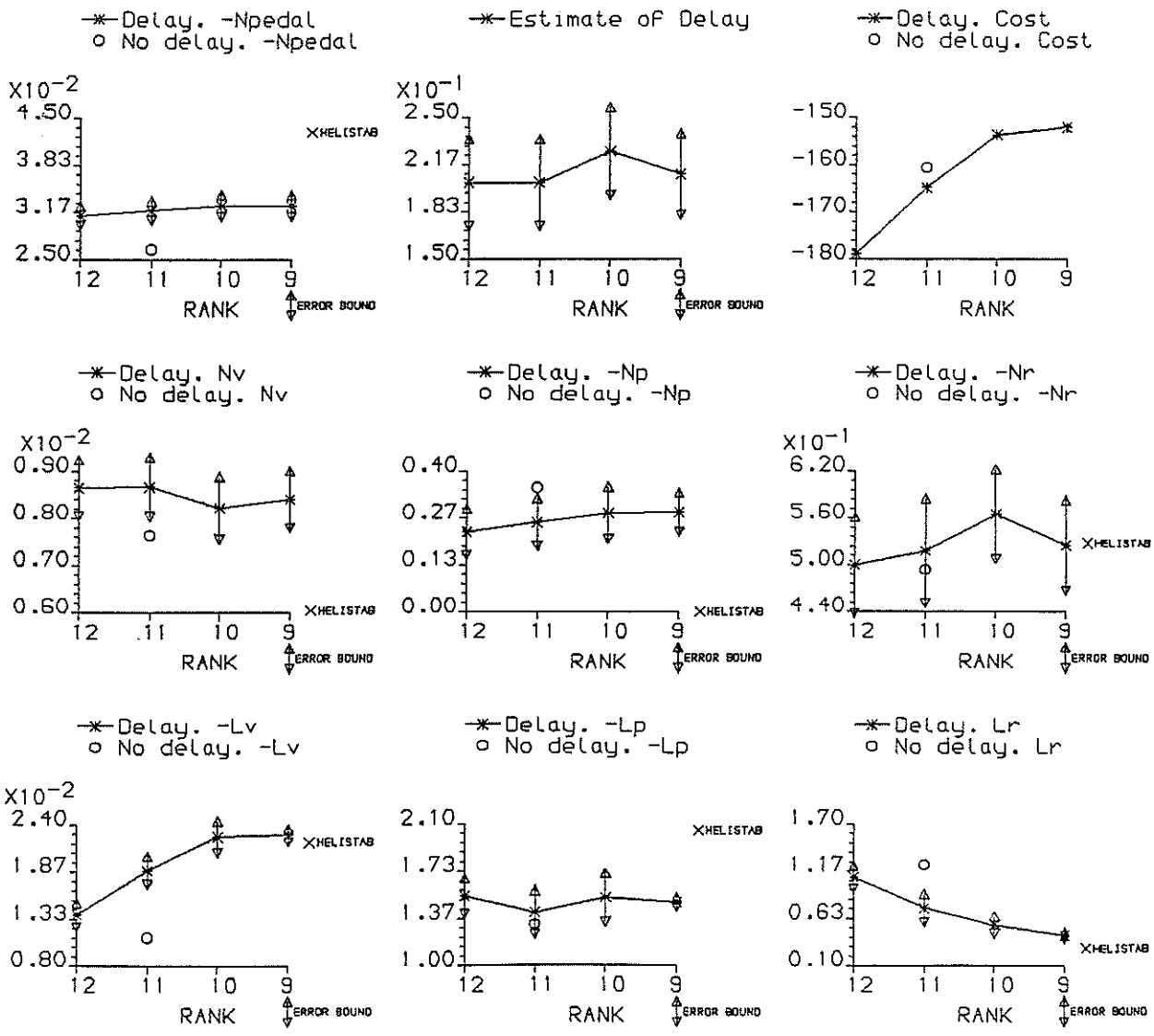

Figure 3. Estimate versus rank of information matrix used. Puma, 100 Kn, run R1201L.

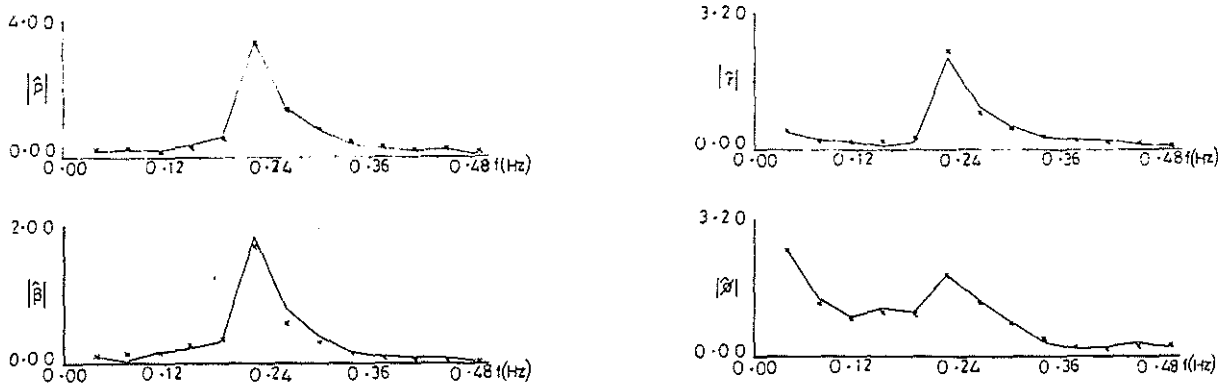

Figure 4. Frequency-domain Fits.
No delay in estimation model.
Puma, 100 Kn, run R1201L.

MEASUREMENT: —
PREDICTION: x

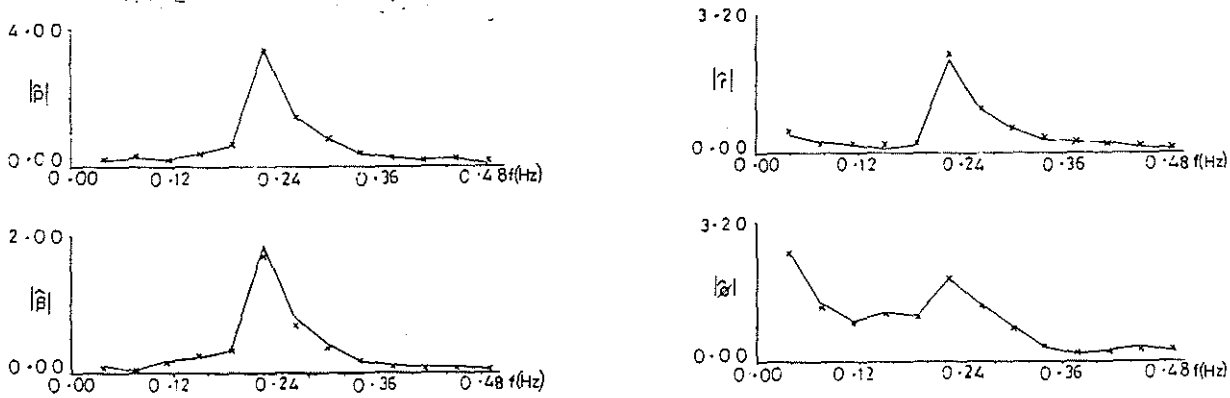

Figure 5. Frequency-domain Fits.
Delay in estimation model.
Puma, 100 Kn, run R1201L.

MEASUREMENT: —
PREDICTION: x

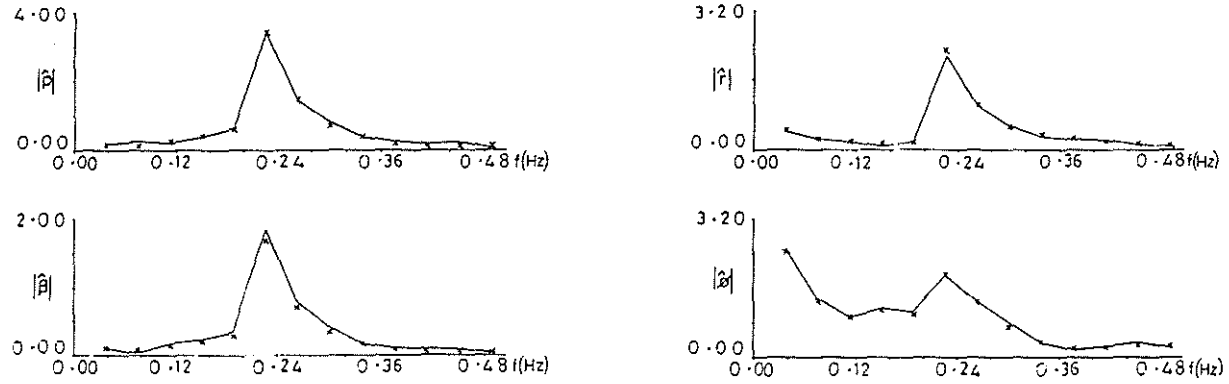

Figure 6. Frequency-domain Fits.
Delay in estimation model, rank-9 solution.
Puma, 100 Kn, run R1201L.

MEASUREMENT: —
PREDICTION: x

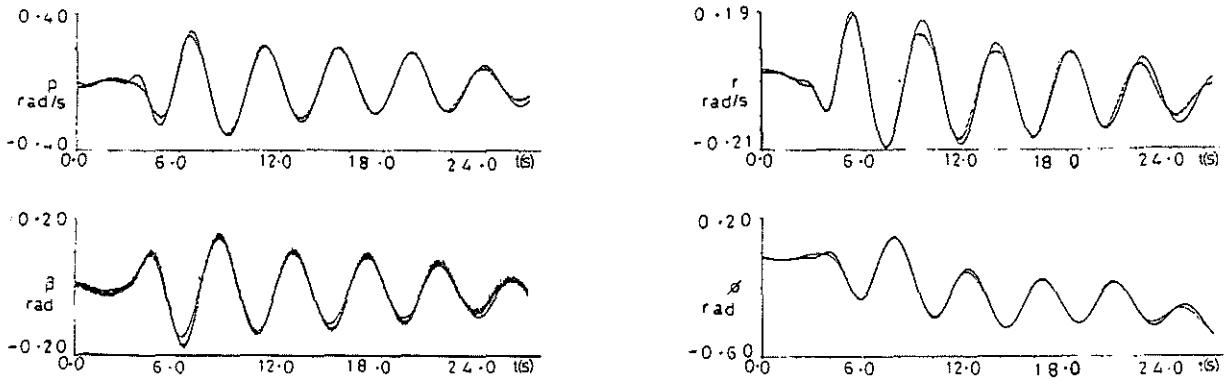

Figure 7. Time-domain Fits.
No delay in estimation model.
Puma, 100 Kn, run R1201L.

MEASUREMENT: ~~~~
PREDICTION: ~

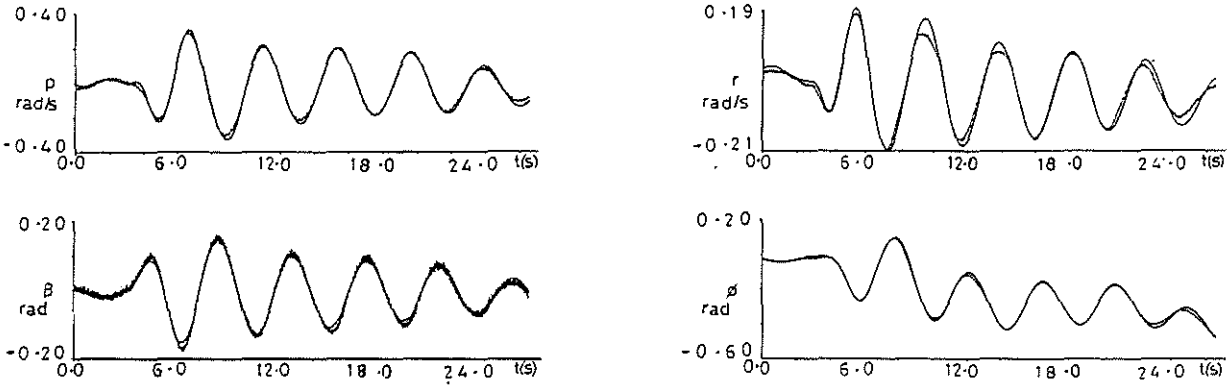

Figure 8. Time-domain Fits.
Delay in estimation model.
Puma, 100 Kn, run R1201L.

MEASUREMENT: ~~~~
PREDICTION: ~

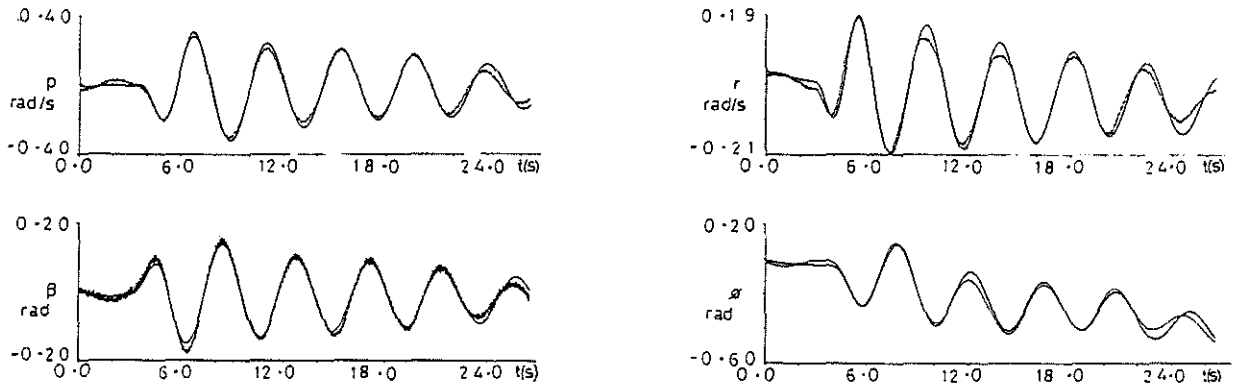

Figure 9. Time-domain Fits.
Delay in estimation model, rank-9 solution.
Puma, 100 Kn, run R1201L.

MEASUREMENT: ~~~~
PREDICTION: ~

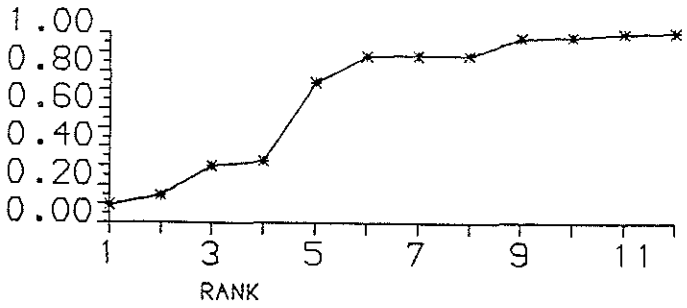

Figure 10. Typical reduction in cost value for use of increasing rank of information matrix. Normalised with respect to full-rank reduction.

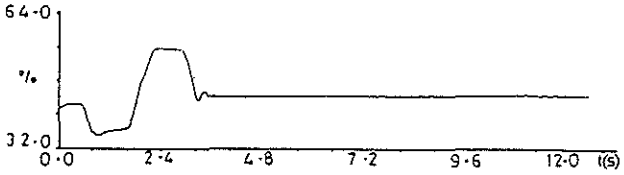

Figure 11. Lateral-cyclic doublet input. Puma, 60 Kn, run R2501R.

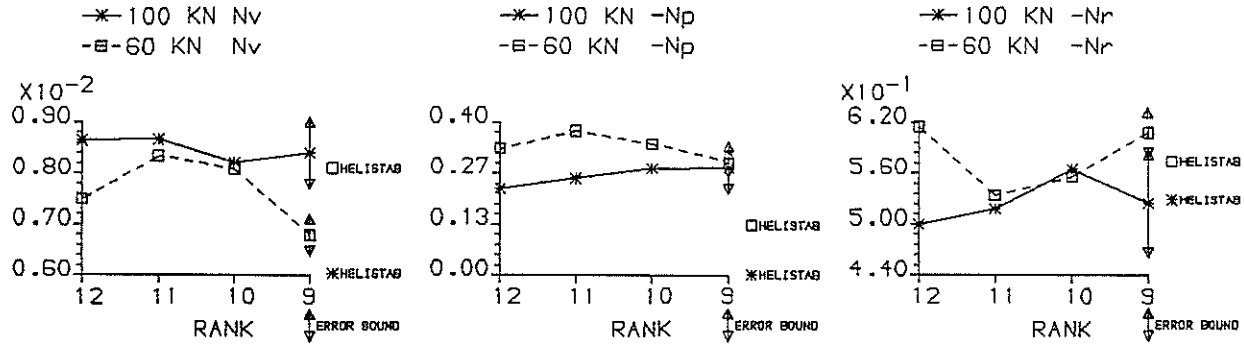

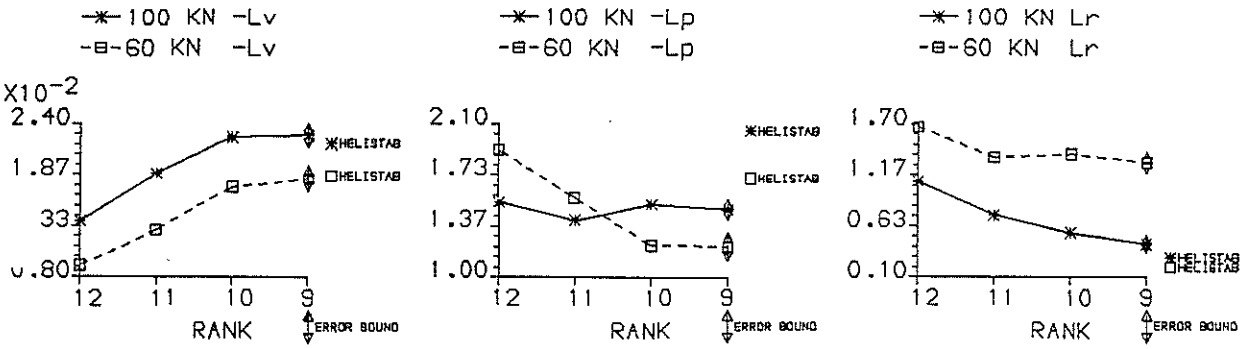

Figure 12 a). Estimate versus rank of information matrix used. Puma, 60 Kn (Lateral-cyclic - run R2501R) & 100 Kn (pedal - run R120'L') comparisons.

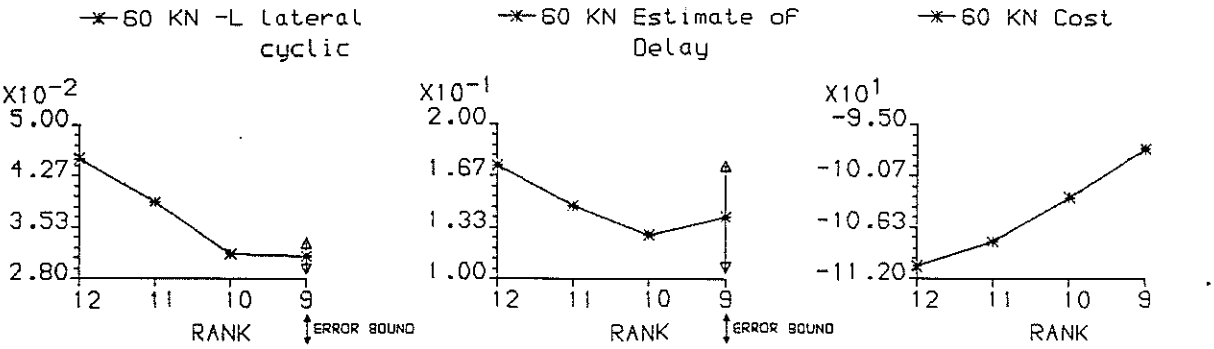

Figure 12 b). Estimate versus rank of information matrix usec. Puma, 60 Kn, run R2501R.

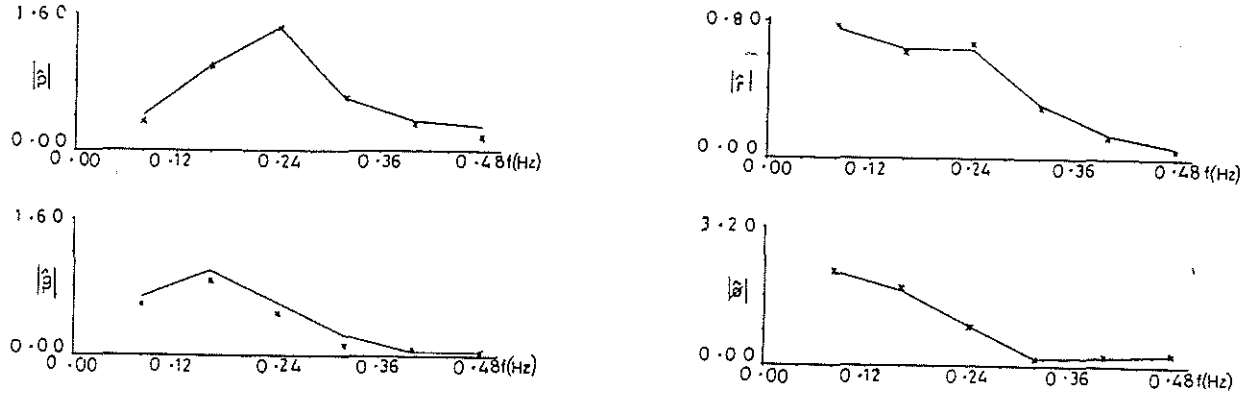

Figure 13. Frequency-domain Fits.
Delay in estimation model, rank-10 solution.
Puma, 60 Kn, run R2501R.

MEASUREMENT: —
PREDICTION: x

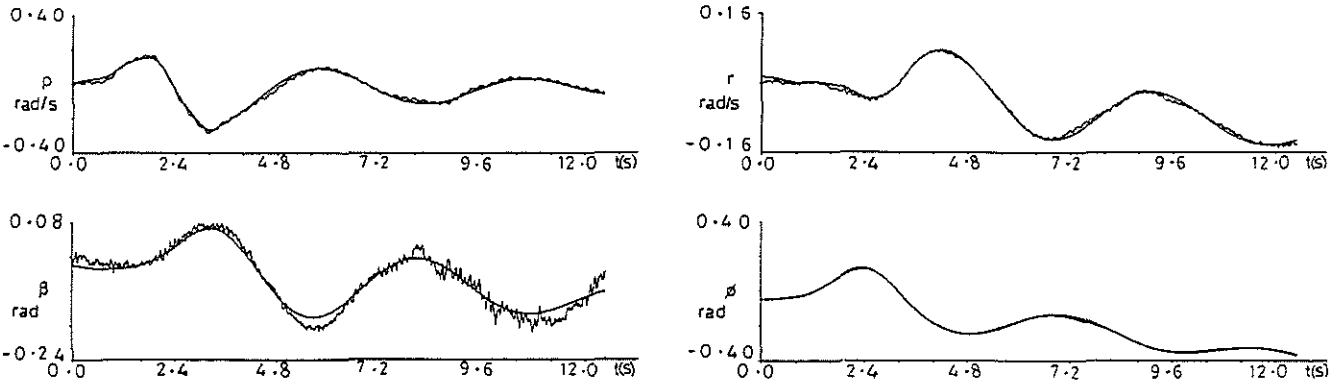

Figure 14. Time-domain Fits.
Delay in estimation model, rank-10 solution.
Puma, 60 Kn, run R2501R.

MEASUREMENT: ~~~
PREDICTION: ~

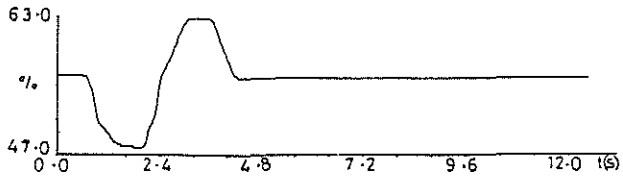

Figure 15. Pedal doublet input, Puma, 60 Kn, run R3401R.

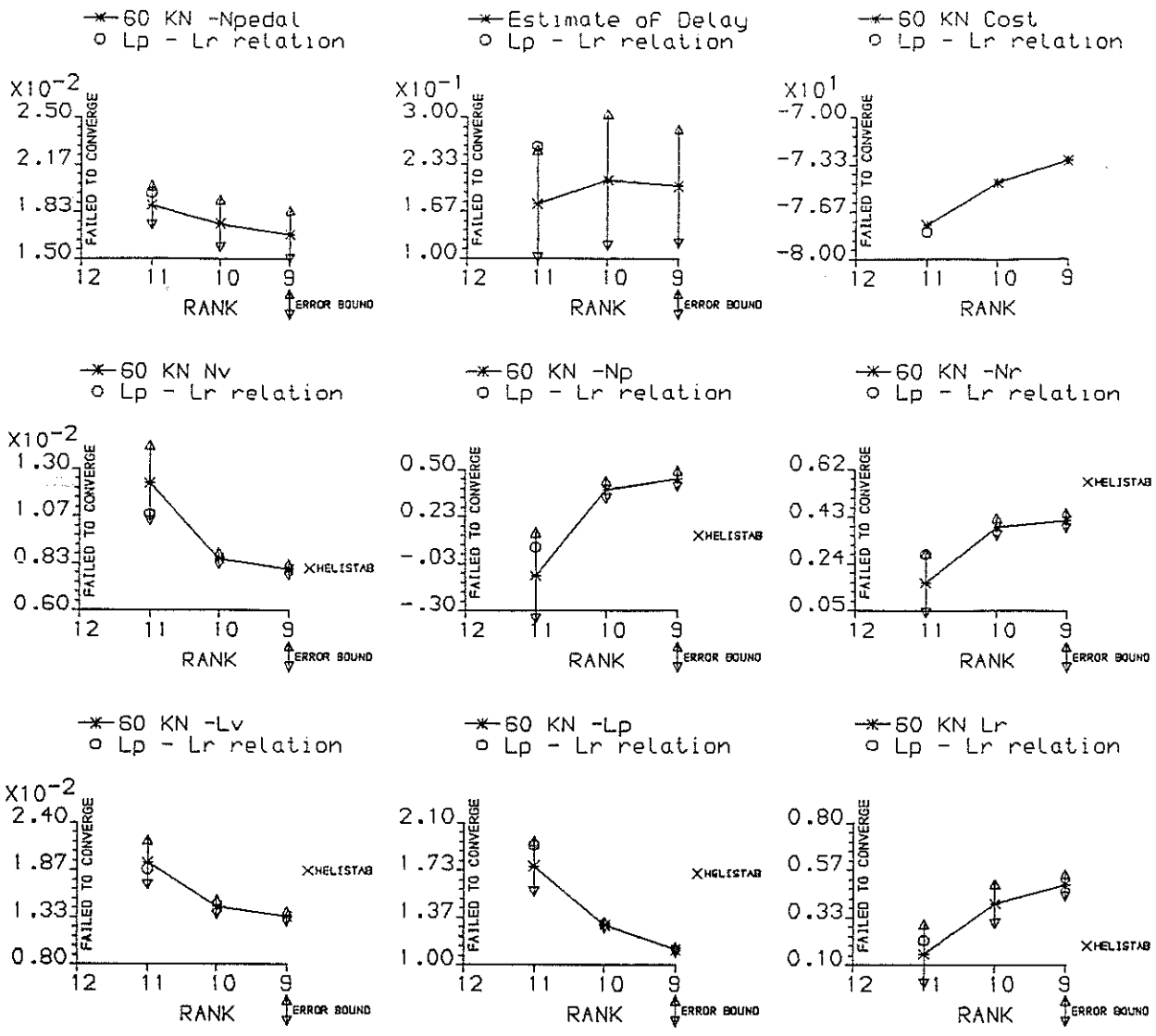

Figure 16. Estimate versus rank of information matrix used. Puma, 60 Kn, run R3401R.

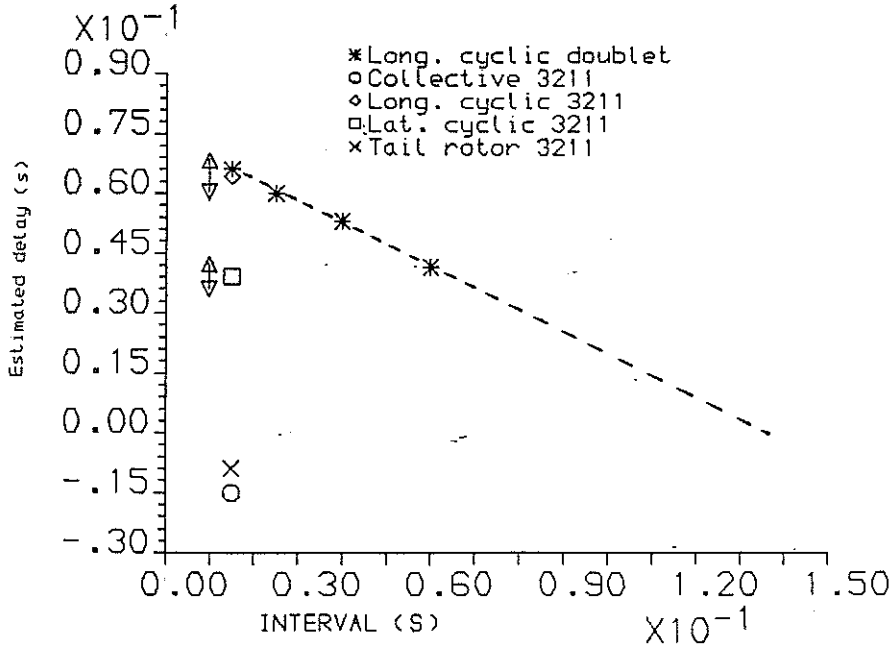

Figure 17. Estimated time delay versus sampling interval using 9 DOF simulated data and a 6 DOF estimation model, HELISTAB.

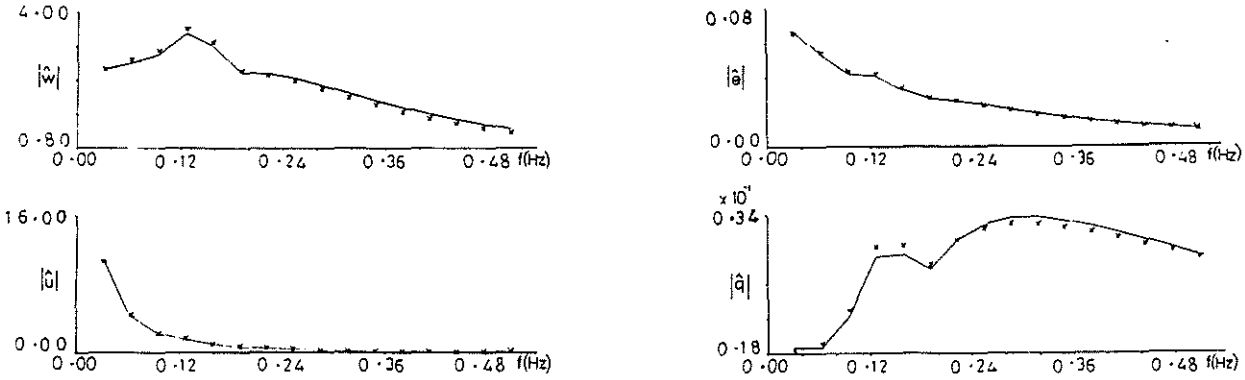

Figure 18. Frequency-domain Fits.
9 DOF data and 6 DOF model with time delay.
HELISTAB, 80 Kn, Longitudinal-cyclic doublet.

MEASUREMENT: —
PREDICTION: x

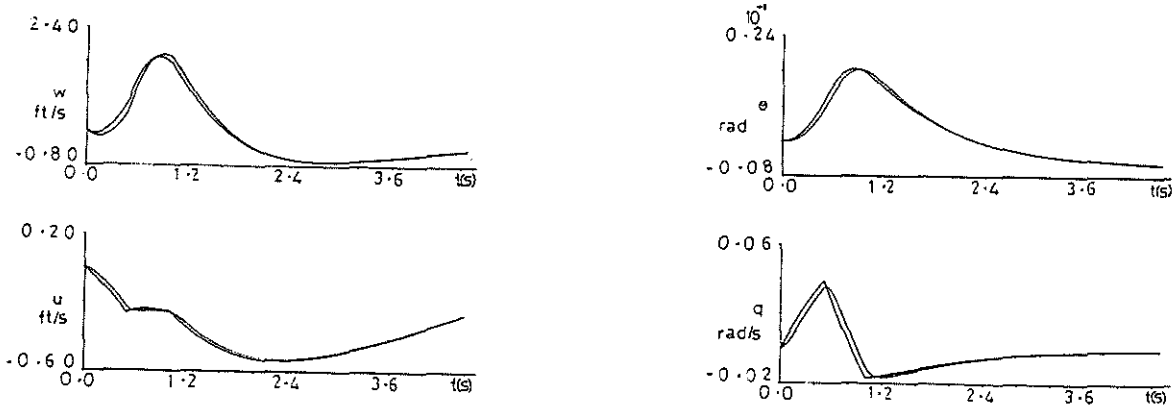

Figure 19 a). Time-domain Fits.
9 DOF data and 6 DOF model without time delay.
HELISTAB, 80 Kn, Longitudinal-cyclic doublet.

9 DOF RESPONSE: ~
6 DOF PREDICTION WITHOUT DELAY: ~

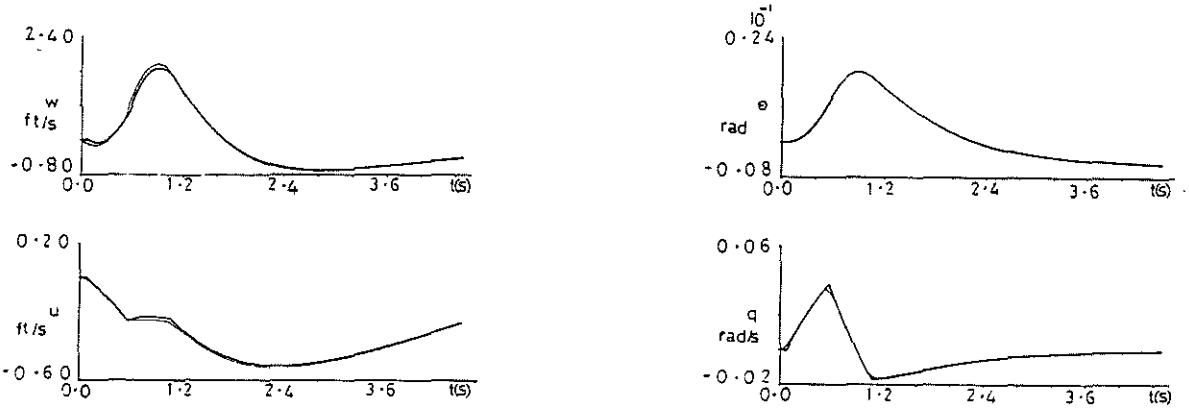

Figure 19 b). Time-domain Fits.
9 DOF data and 6 DOF model with time delay.
HELISTAB, 80 Kn, Longitudinal-cyclic doublet.

9 DOF RESPONSE: ~
6 DOF PREDICTION WITH DELAY: ~